Transaction B: Mechanical Engineering
Vol. 16, No. 1, pp. 75–86
© Sharif University of Technology, February 2009

SCIENTIA IRANICA

Effects of Rotary Inertia and Gyroscopic Momentum on the Flexural Vibration of Rotating Shafts Using Hybrid Modeling

A. Farshidianfar[1] **and S. Soheili**[1,*]

Abstract. *In this paper, the effect of shaft rotation on its natural frequency is investigated. Considering rotary inertia and gyroscopic momentum, the fourth order differential equation representing the flexural vibration of the shaft is solved by the new analytical method. The Distributed Lumped Modeling Technique (DLMT) is applied to obtain the transfer matrix for the distributed elements using the proposed method and for the lumped elements consisting of rotary inertia and gyroscopic effects. The results obtained by this method are compared and verified with the results of two other methods. The effects of shaft diameter, shaft length and disk inertia on the natural frequency are discussed for various speeds. It is shown that, while the new method brings highly accurate results, its simplicity and accuracy provide proper application for use in industrial systems.*

Keywords: *Distributed; Lumped; Modeling; Rotary inertia; Gyroscopic effect.*

INTRODUCTION

The study of the flexural vibration of rotating shafts is an important subject in the design of dynamic systems. The natural frequencies of a rotating shaft actually differ from non-rotating ones, because of the effects of rotary inertia and gyroscopic momentum.

Gyroscopic effects on the critical speed of rotors were studied by Green [1] for the first time. Later, Den Hartog [2] presented a forth degree algebraic equation, including rotary inertia and gyroscopic momentum, for calculation of the whirling speed of a hanger shaft. Considering these effects, Dimentberg [3] provided a review of analytical solutions for various rotor dynamics problems. Further investigation was performed by Eshleman and Eubanks [4] and, also, Rao [5].

Lee et al. [6] presented modal analysis of a rotating shaft, using the Rayleigh beam theory. Lee and Jei [7] solved the equation of motion for a rotating shaft, including gyroscopic moments and rotary inertia, and investigated whirl speeds and mode shapes for different boundary conditions by arranging them in the matrix form.

1. *Department of Mechanical Engineering, Ferdowsi University of Mashhad, Mashhad, Iran.*
*. *Corresponding author. E-mail: sa_so63@stu-mail.um.ac.ir*

Received 2 November 2006; received in revised form 11 July 2007; accepted 1 October 2007

For the modeling and vibration analysis of rotor systems, various methods have been proposed and developed over the years, such as the Finite Element Method (FEM), the Transfer Matrix Method (TMM) and the Distributed-Lumped Modeling Technique (DLMT). The first two methods approximate a rotor system with a finite degree of freedom system, while the latter provides a highly accurate model without approximation.

Nelson's analysis of rotor bearing systems [8], using a finite element method, resulted in a high number of natural frequencies that produced errors, such that the designer could not distinguish the true set of frequencies. Many techniques have been developed to solve the problem, such as the dynamic reduction method by Rouch [9], modal translation by Kim and Lee [10] and component mode synthesis by Glasgow and Nelson [11].

The Transfer Matrix Method (TMM) is another technique proposed by Myklestad [12] and developed by Prohl [13]. This method was later modified by Lund [14]. In this technique, the distributed shaft is divided into 'station' elements, which only possess mass, and 'field' elements, which only possess flexural stiffness but no mass [15]. Further modifications are achieved by a combination of the transfer matrix method and the finite element method [16]. Considering the effects of distributed shafts, Lee et al. [17]

presented a modified transfer matrix method, in which the elements of the distributed parts are frequency dependent.

The Distributed-Lumped Modeling Technique (DLMT) was introduced by Whalley [18] for the first time. This technique was applied by Aleyaasin et al. [19] for computation of the flexural frequencies of shafts using 4×4 matrices. Aleyaasin and Ebrahimi also obtained the frequency response of such systems [20]. Further investigations about the flexural vibration of rotor bearing systems were performed by Aleyaasin et al. (see, for example [21,22]). The distributed-lumped method can be also applied to other systems, such as modeling the torsional [23] and longitudinal vibration and computation of frequency and time responses in forced systems [24]. It can be also applied to fluid systems, as represented by Whalley et al. [25].

Compared with FEM, the DLMT has the following advantages:

1. The order of the transfer matrix for each distributed and lumped element is 4×4. Hence, the order of the transfer matrix of the entire system is also 4×4, while, in FEM, the stiffness matrix of the entire beam is a $2(n+1) \times 2(n+1)$ matrix for the beam with n elements;
2. Displacements, velocities and accelerations are the state variables of FEM, while those of DLMT are displacements, slopes, bending moments and shear forces. In some cases, the 'bending moments' of the entire beam are also required, in addition to the displacements in FEM. In such a case, the DLMT will be more effective than FEM.

Compared with TMM, the DLMT employs an exact solution of the equation of motion to obtain the transfer matrix of the distributed element, therefore, there is no approximation in this method and one can consider the natural frequencies and mode shapes as the exact ones.

This paper studies the effect of gyroscopic momentum and rotary inertia on the natural frequency of rotating shafts. The equation of motion presented by Yamamoto and Ishida [26] is solved using the new method and arranged in the form of distributed-lumped matrices. The results obtained by the hybrid modeling technique (DLMT) are compared with the results of Den Hartog [2] and Behzad et al. [27]. The effect of shaft diameter, shaft length and disk inertia on the first natural frequency is investigated for different rotational speeds and contrasted with cases where gyroscopic momentum and rotary inertia are ignored in the process of modeling. It is also shown how the DLMT can be easily applied to obtain the natural frequencies of complicated systems which brings highly accurate results.

GENERAL DISTRIBUTED-LUMPED MODEL

Generally speaking, systems in the hybrid modeling technique are considered as a combination of two types of element:

1. The distributed element, which is the main part of shafts and rotors, with distributed mass or inertia;
2. The lumped element, which is the supplementary part of shafts and rotors, with concentrated mass or inertia, such as disks, gears, propellers, pulleys and so on.

In this way, a system is considered as a combined set of distributed and lumped elements, in which the final vibration model of the system is obtained by setting the distributed and lumped matrices of different parts and combining them together. Distributed and lumped matrices are formed according to the analytical equations of motion, so this is a highly accurate technique in contrast to other approximate techniques, such as the transfer matrix method, the finite element method and so on. Another advantage of this technique, compared with other analytical methods, is that the continuity conditions between distributed and lumped elements are simply satisfied and it remains only to apply the boundary conditions of the system to the model.

Deriving Transfer Matrix for Distributed Element

According to Figure 1, the main equation of motion for a thin rotating shaft could be expressed as [26,27]:

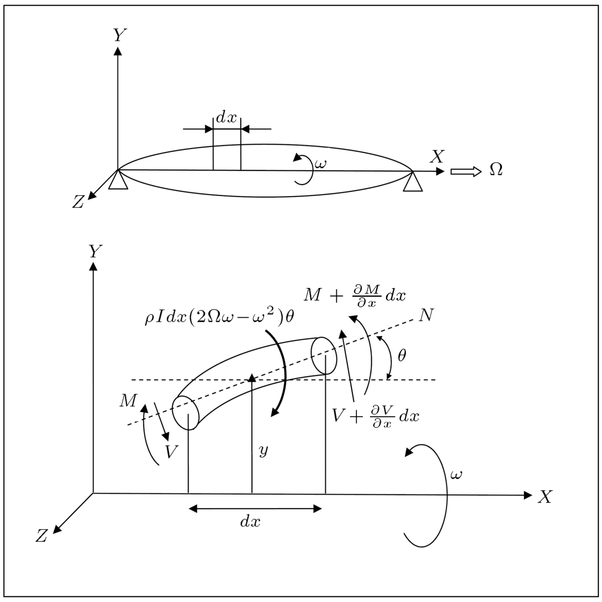

Figure 1. Force and moments of a distributed element.

$$EI\frac{\partial^4 y}{\partial x^4} - \rho A\omega^2 y - \rho I(2\Omega\omega - \omega^2)\frac{\partial^2 y}{\partial x^2} = 0. \tag{1}$$

In order to derive the above equation, the momentum equation for the dx element can be stated in the following form (see Figure 1):

$$\frac{\partial M}{\partial x} + V - \rho I(2\Omega\omega - \omega^2)\theta = 0. \tag{2}$$

The third term in this equation represents rotary inertia and gyroscopic effects, as presented by Den Hartog [2]. Recalling the mechanics of materials, two other relations are obtained as follows:

$$\theta = \frac{\partial y}{\partial x}, \tag{3}$$

$$M = EI\frac{\partial^2 y}{\partial x^2}, \tag{4}$$

and the force equation could be expressed as follows:

$$\frac{\partial V}{\partial x} = -\rho A\omega^2 y. \tag{5}$$

Differentiating Equation 2, with respect to x, and substituting Equations 3, 4 and 5 into it, would result in the equation of motion.

In order to solve Equation 1, y is assumed as a function of x and ω in the following form:

$$y(x,\omega) = ce^{nx}. \tag{6}$$

In this equation, n is a frequency dependent function and c is a constant, calculated according to the boundary conditions. Substitution of this equation in Equation 1 gives:

$$n^4 + an^2 + b = 0, \tag{7}$$

in which a and b are the frequency dependent terms as follows:

$$a = \frac{-\rho}{E}(2\Omega\omega - \omega^2), \tag{8}$$

$$b = \frac{-\rho A}{EI}\omega^2. \tag{9}$$

Therefore, n is obtained by solving Equation 7 in the following form:

$$n = \pm\sqrt{\frac{-a \pm \sqrt{a^2 - 4b}}{2}}, \tag{10a}$$

which can be represented in the complete form as:

$$n = \pm\sqrt{\frac{\rho}{2E}\omega(2\Omega - \omega)}.\sqrt{1 \pm \sqrt{1 + \frac{4A}{I(2\Omega - \omega)^2}}}. \tag{10b}$$

In this way, 4 quantities are obtained for n, hence, $y(x,\omega)$ can be expressed as follows:

$$y = \sum_{i=1}^{4} c_i e^{(n_i x)}. \tag{11}$$

It is clear that there is no approximation in this solution, while it also includes all of the sinusoidal functions. It can be easily applied to find the other parameters. Substitution of this relation into Equations 3 and 4, respectively, gives:

$$\theta = \sum_{i=1}^{4} c_i n_i e^{(n_i x)}, \tag{12}$$

$$M = EI\sum_{i=1}^{4} c_i n_i^2 e^{(n_i x)}. \tag{13}$$

Shear force, V, is obtained by Equation 2 as follows:

$$V = -EI\sum_{i=1}^{4} c_i n_i^3 e^{(n_i x)} + \frac{\rho}{E}(2\Omega\omega - \omega^2)\sum_{i=1}^{4} c_i n_i e^{(n_i x)}. \tag{14}$$

In order to derive the transfer matrix for the distributed element, y, θ, M and V can be expressed in the matrix form as:

$$\begin{Bmatrix} y \\ \theta \\ M \\ V \end{Bmatrix} = [\mathbf{T}(x)][\mathbf{C}], \tag{15}$$

where:

$$[\mathbf{T}(x)] = \begin{bmatrix} e^{(n_1 x)} & e^{(n_2 x)} & e^{(n_3 x)} & e^{(n_4 x)} \\ n_1 e^{(n_1 x)} & n_2 e^{(n_2 x)} & n_3 e^{(n_3 x)} & n_4 e^{(n_4 x)} \\ EIn_1^2 e^{(n_1 x)} & EIn_2^2 e^{(n_2 x)} & EIn_3^2 e^{(n_3 x)} & EIn_4^2 e^{(n_4 x)} \\ (-EIn_1^3 + \frac{\rho}{E}(2\Omega\omega - \omega^2)n_1)e^{(n_1 x)} & (-EIn_2^3 + \frac{\rho}{E}(2\Omega\omega - \omega^2)n_2)e^{(n_2 x)} & (-EIn_3^3 + \frac{\rho}{E}(2\Omega\omega - \omega^2)n_3)e^{(n_3 x)} & (-EIn_4^3 + \frac{\rho}{E}(2\Omega\omega - \omega^2)n_4)e^{(n_4 x)} \end{bmatrix}, \tag{16}$$

and [**C**] is the coefficient matrix as follows:

$$[\mathbf{C}] = \begin{Bmatrix} C_1 \\ C_2 \\ C_3 \\ C_4 \end{Bmatrix}. \tag{17}$$

Ignoring rotary inertia and gyroscopic effects, the equation of motion for a thin shaft would be:

$$EI\frac{\partial^4 y}{\partial x^4} - \rho A\omega^2 y = 0. \tag{18}$$

The function, y, is assumed in the form of Equation 6. Solving the equation of motion by the discussed technique would result in:

$$[\mathbf{T}(x)] = \begin{bmatrix} e^{(n_1x)} & e^{(n_2x)} & e^{(n_3x)} & e^{(n_4x)} \\ n_1e^{(n_1x)} & n_2e^{(n_2x)} & n_3e^{(n_3x)} & n_4e^{(n_4x)} \\ EIn_1^2e^{(n_1x)} & EIn_2^2e^{(n_2x)} & EIn_3^2e^{(n_3x)} & EIn_4^2e^{(n_4x)} \\ -EIn_1^3e^{(n_1x)} & -EIn_2^3e^{(n_2x)} & -EIn_3^3e^{(n_3x)} & -EIn_4^3e^{(n_4x)} \end{bmatrix}, \tag{19}$$

while:

$$n = \beta\exp(\pm i\pi/4) \text{ or } \beta\exp(\pm i3\pi/4), \tag{20}$$

and:

$$\beta = \frac{-\rho A}{EI}\omega^2. \tag{21}$$

Considering the jth element, for the initial point of the shaft (for example, the left side), one should assign $x = 0$ in Equation 15:

$$\begin{Bmatrix} y(0) \\ \theta(0) \\ M(0) \\ V(0) \end{Bmatrix}_j = [\mathbf{T}(0)]_j[\mathbf{C}]_j. \tag{22}$$

Therefore, the coefficient matrix can be expressed as follows:

$$[\mathbf{C}]_j = [\mathbf{T}(0)]_j^{-1}\begin{Bmatrix} y(0) \\ \theta(0) \\ M(0) \\ V(0) \end{Bmatrix}_j. \tag{23}$$

For the shaft with length l, assuming $x = l$, gives:

$$\begin{Bmatrix} y(l) \\ \theta(l) \\ M(l) \\ V(l) \end{Bmatrix}_j = [\mathbf{T}(l)]_j[\mathbf{C}]_j. \tag{24}$$

Substituting Equation 23 in Equation 24 and applying the continuity equation as follows:

$$\begin{Bmatrix} y(0) \\ \theta(0) \\ M(0) \\ V(0) \end{Bmatrix}_j = \begin{Bmatrix} y \\ \theta \\ M \\ V \end{Bmatrix}_{j-1}, \tag{25}$$

would result in:

$$\begin{Bmatrix} y \\ \theta \\ M \\ V \end{Bmatrix}_j = [\mathbf{T}_D]_j\begin{Bmatrix} y \\ \theta \\ M \\ V \end{Bmatrix}_{j-1}, \tag{26}$$

where:

$$[\mathbf{T}_D]_j = [\mathbf{T}(l)]_j[\mathbf{T}(0)]_j^{-1}, \tag{27}$$

which is the main transfer matrix for the distributed element in DLMT.

The complete form of distributed matrix elements using Equation 19 is presented in Appendix A. The elements of the distributed matrix employing Equation 16 are mentioned in Appendix B.

Deriving Transfer Matrix for Lumped Element

According to Figure 2, the relationship between the right and left side of the jth lumped element, such as gear, pulley and so on, regarding rotary inertia and gyroscopic effects, can be expressed in the following form:

$$\begin{aligned} y_j &= y_{j-1}, \\ \theta_j &= \theta_{j-1}, \\ M_j &= M_{j-1} + \rho_d I_d(2\Omega\omega - \omega^2)\theta_{j-1}, \\ V_j &= V_{j-1} - m_d\omega^2 y_{j-1}, \end{aligned} \tag{28}$$

which can be presented in the matrix form as:

$$\begin{Bmatrix} y \\ \theta \\ M \\ V \end{Bmatrix}_j = [\mathbf{T}_L]_j\begin{Bmatrix} y \\ \theta \\ M \\ V \end{Bmatrix}_{j-1}, \tag{29}$$

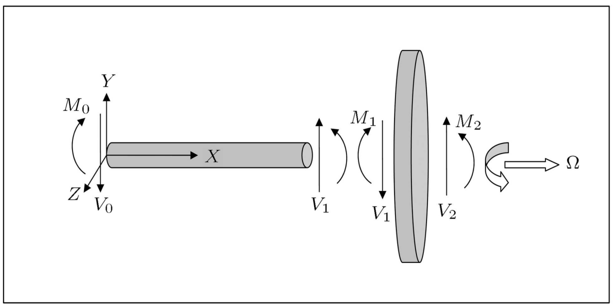

Figure 2. General model of rotating rotor system.

where:

$$[\mathbf{T}_L]_j = \begin{bmatrix} 1 & 0 & 0 & 0 \\ 0 & 1 & 0 & 0 \\ 0 & \rho_d I_d(2\Omega\omega - \omega^2) & 1 & 0 \\ -m_d\omega^2 & 0 & 0 & 1 \end{bmatrix}. \tag{30}$$

ILLUSTRATIVE EXAMPLES

In this section, the methodology outlined previously is applied to a pin-pin and also to a hanger shaft with a disk at its end point (see Figures 2 and 3), which is a simplified model for common industrial systems, such as ship propellers. The effects of shaft diameter, length and disk inertia on the first natural frequency, due to changes in rotational speed, are investigated. The properties of the discussed systems are represented in Tables 1 and 2.

These examples verify the results of the new method and also approve their accuracy. They also show the simplicity of the formulation for the modeling of industrial systems under any boundary conditions. As previously mentioned, the present method can be used for analyzing systems with any number of distributed and lumped elements without an increase in difficulty. It can be also applied to non-uniform shafts with different sections, just by setting the distributed matrices for each section and multiplying them.

The Effect of Shaft Diameter

In order to investigate the effect of shaft diameter on its natural frequency, a simply supported shaft with different diameters ($d = 0.04$, 0.1, 0.2 and 0.4 m) is considered. Shaft properties are mentioned in Table 1. The first natural frequency for this shaft is calculated, according to changes in rotational speed, Ω, up to 50000 r. p. m, and results are shown in Figure 4. In this figure, the percentage of relative change in the first natural frequency, $(\omega - \omega_0)/\omega_0 \times 100$, is plotted versus shaft speed. The continuous line in this figure shows the results presented by Behzad et al. [27] for the mentioned shaft, which is obtained by analytical solution for the first frequency as follows [26,27]:

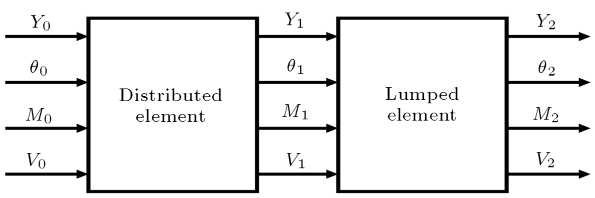

Figure 3. Hybrid model of rotating rotor system.

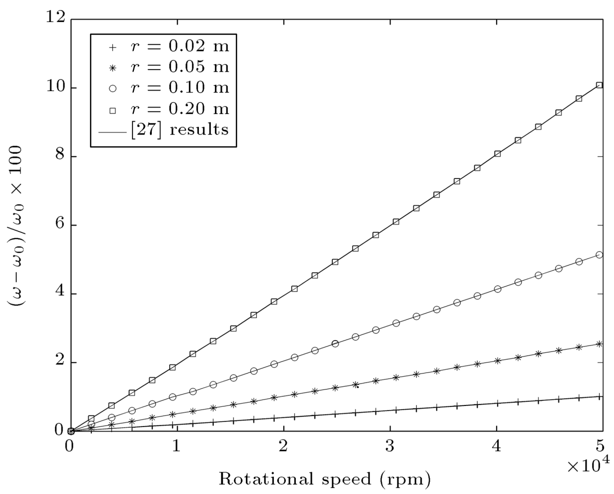

Figure 4. DLMT solution: Relative change of the first natural frequency vs shaft speed for a pin-pin steel rotor.

$$\omega = \frac{\frac{I}{A}\frac{\pi^2}{l^2}\Omega + \sqrt{(\frac{I}{A}\frac{\pi^2}{l^2}\Omega)^2 + \frac{EI}{\rho A}(1 + \frac{I}{A}\frac{\pi^2}{l^2})\frac{\pi^4}{l^4}}}{1 + \frac{I}{A}\frac{\pi^2}{l^2}}. \tag{31}$$

Considering this figure, it can be seen that there is good agreement between the results of these two methods, therefore; it also approves the accuracy of the new method. Natural frequencies in these equations represent 'Forward Whirling' modes, which are cases in which the direction of ω and Ω are the same. Forward whirling is more common in practice and considered everywhere in this paper as the vibration mode. It is clear that increasing the shaft diameter would increase gyroscopic momentum and rotary inertia, which results in greater natural frequencies.

The Effect of Disk

In this section, the capability of DLMT, as a powerful and accurate method for the free vibration analysis of complicated beams, is investigated. The assumed system, as shown in Figure 2, is a rotating cantilever shaft with an end disk. The system properties are

Table 1. Properties of the pin-pin shaft.

Shaft Length l	1 m
Shaft Diameter d_{shaft}	0.04, 0.1, 0.2, 0.4 m
Density of Shaft Material ρ	7800 kg/m^3
Modulus of Elasticity for Shaft E	207 GPa
Poisson Ratio v	0.33

Table 2. Properties of the cantilever shaft.

Shaft Length l	0.4 m
Shaft Diameter d_{shaft}	0.08 m
Density of Shaft Material ρ	7800 kg/m^3
Modulus of Elasticity for Shaft E	200 GPa
Shear Modulus of Shaft G	80 GPa
Mass of Disk	100 kg
Moment of Inertia for Disk	5.33

presented in Table 2. The distributed-lumped model of this system, as shown in Figure 3, can be represented in the following form:

$$\begin{Bmatrix} y \\ \theta \\ M \\ V \end{Bmatrix}_2 = [\mathbf{T}] \begin{Bmatrix} y \\ \theta \\ M \\ V \end{Bmatrix}_0, \tag{32}$$

where $[\mathbf{T}]$ in this equation is obtained as follows:

$$[\mathbf{T}] = [\mathbf{T}_L][\mathbf{T}_D]. \tag{33}$$

Equation 32 can be expanded into four equations in the following form:

$$y_2 = T_{11}y_0 + T_{12}\theta_0 + T_{13}M_0 + T_{14}V_0, \tag{34}$$

$$\theta_2 = T_{21}y_0 + T_{22}\theta_0 + T_{23}M_0 + T_{24}V_0, \tag{35}$$

$$M_2 = T_{31}y_0 + T_{32}\theta_0 + T_{33}M_0 + T_{34}V_0, \tag{36}$$

$$V_2 = T_{41}y_0 + T_{42}\theta_0 + T_{43}M_0 + T_{44}V_0. \tag{37}$$

For this system, boundary conditions would be $y_0 = \theta_0 = 0$ for the fixed end (left side), and $M_2 = V_2 = 0$ for the free end (right side) of the model. Hence, Equations 36 and 37 can be expressed as follows:

$$T_{33}M_0 + T_{34}V_0 = 0, \tag{38}$$

$$T_{43}M_0 + T_{44}V_0 = 0. \tag{39}$$

In order to avoid a trivial solution, the presented determinant should be zero:

$$\det \begin{bmatrix} T_{33} & T_{34} \\ T_{43} & T_{44} \end{bmatrix} = 0. \tag{40}$$

Equation 40 is the main frequency equation for the assumed model, and all the natural frequencies are obtained by solving it.

In order to verify the results, the first natural frequency obtained from the above method is compared with the results obtained from the following frequency equation, presented by Den Hartog [2]:

$$F^4 - 2SF^3 + \frac{D+1}{D(e-1)}F^2 - \frac{2S}{e-1}F - \frac{1}{D(e-1)} = 0. \tag{41}$$

For the mentioned system, with $D = 1$ and $e = 0.75$, Equation 41 is reduced as follows:

$$F^4 - 2SF^3 - 8F^2 + 8SF + 4 = 0. \tag{42}$$

There are several ways to solve the above equation; one is to take a value for F and solve the linear equation in S.

Figure 5 shows the results obtained from the above equation and the two distributed-lumped models as F versus S. For the DLMT results, in one case, rotary inertia and gyroscopic moment are considered in both distributed and lumped elements, while, in the other case, they are ignored in the distributed element. It is clear that there is no considerable difference between these two methods, which approves the new applied method. It should be noted that the distributed-lumped method is much easier in practice, and all frequencies can be calculated by this method. The 45-degree dotted line shows the case, in which $\omega = \Omega$. The intersection of this line with the frequency curve shows the critical speed of the system.

Since the shaft is thin and short, rotary inertia and gyroscopic momentum have the least effects, hence, regarding or ignoring them would result in no considerable difference in the first natural frequency. In order to examine these effects, Figure 6 is plotted for the same system with $d = 0.3$ m. It can be seen that the mentioned effects increase the first natural frequency as expected. The deviation from Den Hartog's solution (Equation 41) is because of the nature of this equation, which ignores the inertia force, rotary inertia and gyroscopic effects for the shaft. In other words, it regards the shaft as a lumped element, only possessing

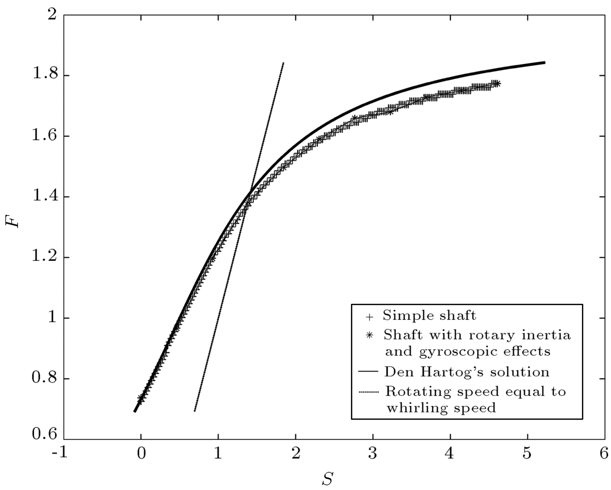

Figure 5. Relative change of the first natural frequency vs shaft speed for a hanger shaft (with $l = 0.4$ m, $d = 0.08$ m and 5.33 kgm^2 disk inertia).

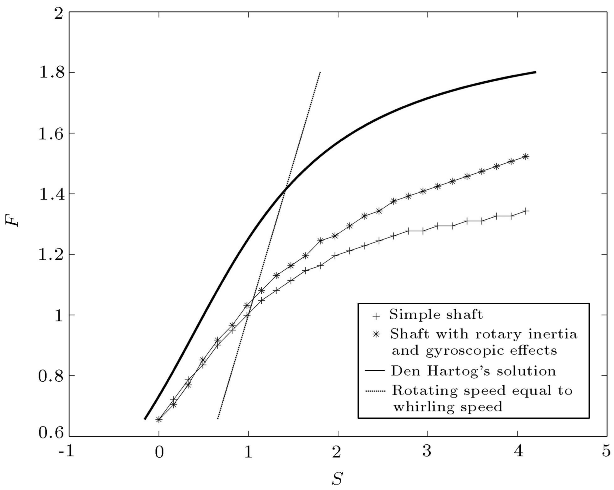

Figure 6. Shaft effect: Relative change of the first natural frequency vs shaft speed for a hanger shaft (with $l = 0.4$ m, $d = 0.3$ m and 5.33 kgm^2 disk inertia).

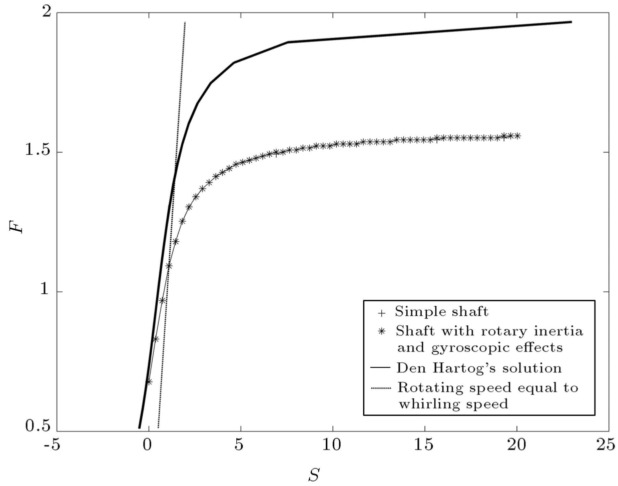

Figure 7. Shaft and disk effect: Relative change of the first natural frequency vs shaft speed for a hanger shaft (with $l = 4$ m, $d = 0.08$ m and 533.33 kgm^2 disk inertia).

mechanical properties [2]. It is also clear that rotary inertia and gyroscopic effects are negligible for lower rotational speeds.

Table 3 shows the approximate range of rotational velocity and the first natural frequency. Comparing Figures 5 and 6, it is clear that increasing the diameter of the shaft would increase the frequencies.

Figure 7 shows the first natural frequency for the shaft with $l = 4$ m and $d = 0.08$ m. Disk inertia is increased to 533.33 kgm^2, such that $D = 1$, in this case. Since the shaft is thin and short, the results are similar to those explained in Figure 5, that is, the effects of rotary inertia and gyroscopic momentum are insignificant. However, there is a deviation from Den Hartog's results, because of neglecting distributed properties.

Figure 8 shows the results for the above shaft, except that disk inertia is reduced to 5.33 kgm^2, such that $D = 0.01$, in this case. Compared with the previous figure, the same pattern is repeated here, except that the scale of S is one hundred times greater, that is, in this case, the amount of rotational speed is one hundred times greater. Therefore, the frequency is not so sensitive, in contrast to the previous case, and its changes are less than before.

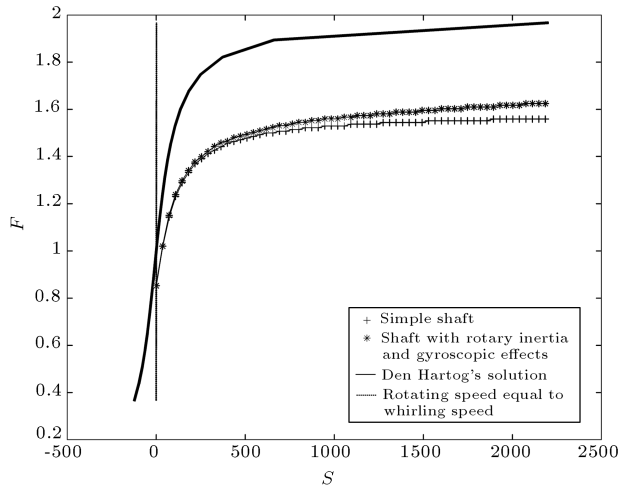

Figure 8. Shaft and disk effect: Relative change of the first natural frequency vs shaft speed for a hanger shaft (with $l = 4$ m, $d = 0.08$ m and 5.33 kgm^2 disk inertia).

According to Table 3, it is clear that increasing the disk inertia would increase the natural frequency sensitivity to the changes in rotational velocity. While the natural frequency has nearly the same domain as in Figures 7 and 8, the rotational velocity changes in a

Table 3. The approximate range of changes.

Figure Number	l	d	Disk Inertia	D	Approximate Range of ω	Approximate Range of Ω
5	0.4	0.08	5.33	1	312-755	0-1736
6	0.4	0.3	5.33	1	3968-9158	0-24421
7	4	0.08	533.33	1	9-21	0-274
8	4	0.08	5.33	0.01	12-22	0-27458
9	4	0.8	533.33	1	1222-1647	0-3432

greater domain for the system with smaller disk inertia. That is, greater disk inertia would change the natural frequency more rapidly.

Comparison of Figures 5 and 8 show the effect of shaft length on natural frequencies. As expected, the longer shaft has a smaller natural frequency and is less sensitive to the changes of rotational velocity.

Figure 9 is plotted for the shaft with $l = 4$ m, $d = 0.8$ m and the disk with a 533.33 kgm^2 moment of inertia. It can be seen that there is a significant difference between the two distributed-lumped models, which is caused by rotary inertia and gyroscopic effects. It also shows that these effects are negligible at lower speeds, while they are predominant at higher frequencies. There is also a considerable deviation from Den Hartog's solution, which was also expected.

Figures 7 and 9 show the effect of shaft diameter on the natural frequency in long shafts. Regarding Table 3, it can be seen that the shaft with greater diameter would have greater natural frequency.

These examples approve the accuracy and simplicity of the hybrid modeling technique, while one can extend this method to also model complicated systems. It should be noted that, while the Den Hartog solution provides only two natural frequencies and can be applied to very limited cases, all the natural frequencies of a vibrating system can be obtained by employing the distributed lumped modeling technique, which can also be applied for modeling systems with any number of distributed and lumped elements.

CONCLUSIONS

In this paper, a new solution for the equation of motion of a rotating shaft, considering rotary inertia and gyroscopic effects, is presented. Combined with a distributed-lumped modeling technique, it provides a highly accurate model for vibrating systems. It is shown that, since analytical techniques are used and the results are of high accuracy, the method can be easily applied for complicated systems, consisting of a various number of distributed and lumped elements under any boundary conditions. In order to verify the solution, the results obtained by this method are compared with the results of Behzad and Bastami [27] and Den Hartog [2], which were obtained by employing other techniques, and good conformity is achieved. The effect of shaft diameter, shaft length and disk inertia on the first natural frequency is investigated for various speeds, and the results are compared with those of Den Hartog's solution. Figures 5 and 7 show that, for slender shafts and at lower speeds, rotary inertia and gyroscopic effects are ignorable and the simple model (without these effects) can be applied. Inversely, in thick shafts or at higher speeds, the mentioned effects bring about a great increment in the first natural frequency, as shown in Figures 6 and 9.

However, the frequencies obtained by the distributed-lumped method are always less than the Den Hartog solution, because inertia force, rotary inertia and gyroscopic effects are neglected in the latter method. It means that the Den Hartog method could be used as an upper bound for the natural frequency of such systems.

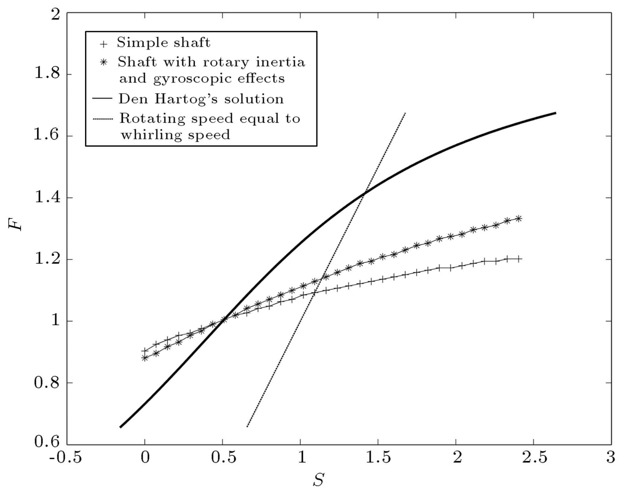

Figure 9. Shaft and disk effect: Relative change of the first natural frequency vs shaft speed for a hanger shaft (with $l = 4$ m, $d = 0.8$ m and 533.33 kgm^2 disk inertia).

NOMENCLATURE

a	frequency dependent coefficient in the equation of motion
A	the cross sectional area of shaft
b	frequency dependent coefficient in the equation of motion
c	constant in the assumed displacement function
$[\mathbf{C}]$	the coefficient matrix
d	shaft diameter
D	the disk effect in SnDen Hartog's formula $\left(D = \frac{I_d \alpha_{22}}{m\alpha_{11}}\right)$
e	the elastic coupling in SnDen Hartog's formula $\left(e = \frac{\alpha_{12}^2}{\alpha_{11}\alpha_{22}}\right)$
E	modulus of elasticity for shaft
F	the dimensionless frequency in SnDen Hartog's formula $(F = \omega\sqrt{\alpha_{11} m})$
G	Shear modulus of shaft
I	the transverse moment of inertia for shaft
I_d	the transverse moment of inertia for disk
j	element numerator

l	shaft length
m_d	mass of disk
M	bending moment
n	frequency dependent coefficient in the assumed displacement function
S	the dimensionless speed in SnDen Hartog's formula ($S = \Omega\sqrt{\alpha_{11}m}$)
$[\mathbf{T}(x)]$	the transfer matrix
$[\mathbf{T}_D]$	transfer matrix for the distributed element
$[\mathbf{T}_L]$	transfer matrix for the lumped element
V	Shear force
y	displacement function
α_{11}	coefficient in SnDen Hartog's formula $\left(\alpha_{11} = \frac{l^3}{3EI}\right)$
α_{12}	coefficient in SnDen Hartog's formula $\left(\alpha_{12} = \frac{l^2}{2EI}\right)$
α_{22}	coefficient in SnDen Hartog's formula $\left(\alpha_{22} = \frac{l}{EI}\right)$
ρ	density of shaft material
ρ_d	density of disk material
β	non-dimensional coefficient in the Euler-Bernoulli beam theory
ω	the frequency of vibration
ω_0	the first natural frequency
Ω	the rotational speed of shaft
θ	the slope function

REFERENCES

1. Green, R.B. "Gyroscopic effects on the critical speed of flexible rotors", *Trans. ASME*, **70**, pp. 369-376 (1948).
2. Den Hartog, J.P., *Mechanical Vibrations*, McGraw-Hill Inc. (1956).
3. Dimentberg, F.M., *Flexural Vibrations of Rotating Shafts*, Butterworth, London (1961).
4. Eshleman, R.L. and Eubanks, R.A. "On the critical speeds of a continuous shaft-disk system", *J. of Engrg. Indust.*, **80**(4), pp. 645-652 (1967).
5. Rao, S.S., *Rotor Dynamics*, John Wiley and Sons Inc., New York (1983).
6. Lee, C.W., Katz, R., Ulsoy, A.G. and Scott, R.A. "Modal analysis of a distributed-parameter rotating shaft", *J. of Sound and Vib.*, **122**(1), pp. 119-130 (1988).
7. Lee, C.W. and Jei, Y.G. "Modal analysis of continuous rotor-bearing systems", *J. of Sound and Vib.*, **126**(2), pp. 345-361 (1988).
8. Nelson, H.D. and McVaugh, T. "The dynamics of rotor bearing systems using finite elements", *J. of Engrg. Indust.*, **98**, pp. 593-600 (1976).
9. Rouch, K.E. and Kao, J.S. "Dynamic reduction in rotor dynamics by the finite element method", *J. of Mech. Design*, **102**, pp 360-367 (1980).
10. Kim, Y.D. and Lee, C.W. "Finite element analysis of rotor bearing systems using a modal transformation matrix", *J. of Sound and Vib.*, **111**(3), pp. 441-456 (1986).
11. Glasgow, D.A. and Nelson, H.D. "Stability analysis of rotor-bearing systems using component mode synthesis", *J. of Mech. Design*, **102**, pp. 353-359 (1980).
12. Myklestad, N.O. "A new method of calculating natural modes of uncoupled bending vibration of airplane wings and other types of beam", *J. of Aerosol Sci.*, **11**, pp. 153-162 (1944).
13. Prohl, M.A. "A general method for calculating critical speeds of flexible rotors", *J. of Appl. Mech.*, **12**, pp. 142-148 (1945).
14. Lund, J.W. "Stability and damped critical speeds of a flexible rotor in fluid-film bearings", *J. of Engrg. Indust.*, pp. 509-517 (1974).
15. Meirovitch, L., *Fundamentals of Vibration*, McGraw-Hill Inc., Singapore (2001).
16. Firoozian, R. and Zhu, H. "A hybrid method for the vibration analysis of rotor-bearing systems", *Proc. of IMechE*, **205**(C), pp. 131-137 (1991).
17. Lee, A.C., Kang Y. and Liu, S.L. "A modified transfer matrix method for linear rotor-bearing systems", *ASME J. of Appl. Mech.*, **58**, pp. 776-783 (1991).
18. Whalley, R. "The response of distributed-lumped parameter systems", *Proc. of IMechE.*, **202**(C6), pp. 421-428 (1988).
19. Aleyaasin, M., Ebrahimi, M. and Whalley R., "Flexural vibration of rotating shafts by frequency domain hybrid modeling", *J. of Comput. and Struct.*, **79**, pp. 319-331 (2001).
20. Aleyaasin, M. and Ebrahimi, M. "Hybrid modeling for analysis and identification of rotors", *J. of Comput. Methods in Appl. Mech. and Engrg.*, **182**, pp. 163-176 (2000).
21. Aleyaasin, M., Ebrahimi, M. and Whalley, R. "Vibration analysis of distributed-lumped rotor systems", *J. of Comput. Methods in Appl. Mech. and Engrg.*, **189**, pp. 545-588 (2000).
22. Aleyaasin, M., Ebrahimi, M. and Whalley, R. "Multivariable hybrid models for rotor-bearing systems", *J. of Sound and Vib.*, **233**(5), pp. 835-856 (2000).
23. Farshidianfar, A., Dalir, H. and Shayan Amin, S. "Frequency investigation of rotating rotors torsional vibration using hybrid modeling technique", *Proc. of Annu. (Int.) Conf. of Manuf. Engrg.*, Amirkabir University, Tehran (2003).
24. Tahani, M. and Soheili, S. "Frequency and time response of rotors longitudinal vibration using hybrid modeling", *13th Annu. (Int.) Mech. Engrg. Conf.*, Isfahan (2005).

25. Whalley, R., Barlett, H. and Ebrahimi, M. "Analytical solution of distributed-lumped parameter network models", *Proc. of IMechE*, **211**(I), pp. 203-218 (1997).

26. Yamamoto, T. and Ishida, Y., *Linear and Nonlinear Rotordynamics: A Modern Treatment with Applicayions*, John Wiley and Sons Inc. (2001).

27. Behzad, M. and Bastami, A.R. "Effect of centrifugal force on natural frequency of lateral vibration of rotating shafts", *J. of Sound and Vib.*, **274**, pp. 985-995 (2004).

APPENDIX A

Considering Equation 27, the main transfer matrix for a shaft with length x could be stated as:

$$[\mathbf{T}] = [\mathbf{T}(x)][\mathbf{T}(0)]^{-1}. \tag{A1}$$

Assuming Relation 19 as the transfer matrix for the distributed element (shaft), in which rotary inertia and gyroscopic effects are ignored, the main transfer matrix would have the following elements:

$$T_{11} = -\frac{e^{n_1x}n_2n_3n_4}{k_4} + \frac{e^{n_2x}n_1n_3n_4}{k_3} - \frac{e^{n_3x}n_1n_2n_4}{k_2} + \frac{e^{n_4x}n_1n_2n_3}{k_1},$$

$$T_{12} = \frac{e^{n_1x}k_8}{k_4} - \frac{e^{n_2x}k_7}{k_3} + \frac{e^{n_3x}k_6}{k_2} - \frac{e^{n_4x}k_5}{k_1},$$

$$T_{13} = \frac{1}{EI}\left(-\frac{e^{n_1x}(n_2+n_3+n_4)}{k_4} + \frac{e^{n_2x}(n_1+n_3+n_4)}{k_3} - \frac{e^{n_3x}(n_1+n_2+n_4)}{k_2} + \frac{e^{n_4x}(n_1+n_2+n_3)}{k_1}\right),$$

$$T_{14} = \frac{1}{EI}(-\frac{e^{n_1x}}{k_4} + \frac{e^{n_2x}}{k_3} - \frac{e^{n_3x}}{k_2} + \frac{e^{n_4x}}{k_1}),$$

$$T_{21} = n_1n_2n_3n_4\left(-\frac{e^{n_1x}}{k_4} + \frac{e^{n_2x}}{k_3} - \frac{e^{n_3x}}{k_2} + \frac{e^{n_4x}}{k_1}\right),$$

$$T_{22} = \frac{n_1e^{n_1x}k_8}{k_4} - \frac{n_2e^{n_2x}k_7}{k_3} + \frac{n_3e^{n_3x}k_6}{k_2} - \frac{n_4e^{n_4x}k_5}{k_1},$$

$$T_{23} = \frac{1}{EI}\left(-\frac{n_1e^{n_1x}(n_2+n_3+n_4)}{k_4} + \frac{n_2e^{n_2x}(n_1+n_3+n_4)}{k_3} - \frac{n_3e^{n_3x}(n_1+n_2+n_4)}{k_2} + \frac{n_4e^{n_4x}(n_1+n_2+n_3)}{k_1}\right),$$

$$T_{24} = \frac{1}{EI}\left(-\frac{n_1e^{n_1x}}{k_4} + \frac{n_2e^{n_2x}}{k_3} - \frac{n_3e^{n_3x}}{k_2} + \frac{n_4e^{n_4x}}{k_1}\right),$$

$$T_{31} = EIn_1n_2n_3n_4\left(-\frac{n_1e^{n_1x}}{k_4} + \frac{n_2e^{n_2x}}{k_3} - \frac{n_3e^{n_3x}}{k_2} + \frac{n_4e^{n_4x}}{k_1}\right),$$

$$T_{32} = EI\left(\frac{n_1^2e^{n_1x}k_8}{k_4} - \frac{n_2^2e^{n_2x}k_7}{k_3} + \frac{n_3^2e^{n_3x}k_6}{k_2} - \frac{n_4^2e^{n_4x}k_5}{k_1}\right),$$

$$T_{33} = -\frac{n_1^2e^{n_1x}(n_2+n_3+n_4)}{k_4} + \frac{n_2^2e^{n_2x}(n_1+n_3+n_4)}{k_3} - \frac{n_3^2e^{n_3x}(n_1+n_2+n_4)}{k_2} + \frac{n_4^2e^{n_4x}(n_1+n_2+n_3)}{k_1},$$

$$T_{34} = -\frac{n_1^2e^{n_1x}}{k_4} + \frac{n_2^2e^{n_2x}}{k_3} - \frac{n_3^2e^{n_3x}}{k_2} + \frac{n_4^2e^{n_4x}}{k_1},$$

$$T_{41} = EIn_1n_2n_3n_4\left(\frac{n_1^2e^{n_1x}}{k_4} - \frac{n_2^2e^{n_2x}}{k_3} + \frac{n_3^2e^{n_3x}}{k_2} - \frac{n_4^2e^{n_4x}}{k_1}\right),$$

$$T_{42} = EI\left(-\frac{n_1^3e^{n_1x}k_8}{k_4} + \frac{n_2^3e^{n_2x}k_7}{k_3} - \frac{n_3^3e^{n_3x}k_6}{k_2} + \frac{n_4^3e^{n_4x}k_5}{k_1}\right),$$

$$T_{43} = -\frac{n_1^3e^{n_1x}(n_2+n_3+n_4)}{k_4} + \frac{n_2^3e^{n_2x}(n_1+n_3+n_4)}{k_3} - \frac{n_3^3e^{n_3x}(n_1+n_2+n_4)}{k_2} + \frac{n_4^3e^{n_4x}(n_1+n_2+n_3)}{k_1},$$

$$T_{44} = \frac{n_1^3e^{n_1x}}{k_4} - \frac{n_2^3e^{n_2x}}{k_3} + \frac{n_3^3e^{n_3x}}{k_2} - \frac{n_4^3e^{n_4x}}{k_1}, \tag{A2}$$

in which k_1 to k_8 are the following relations:

$$k_1 = n_1n_2n_3 - n_4(n_1n_2 + n_2n_3 + n_1n_3) + n_4^2(n_1 + n_2 + n_3) - n_4^3,$$

$$k_2 = -n_1n_2n_4 + n_3(n_1n_2 + n_2n_4 + n_1n_4) - n_3^2(n_1 + n_2 + n_4) + n_3^3,$$

$$k_3 = n_1n_3n_4 - n_2(n_1n_3 + n_3n_4 + n_1n_4) + n_2^2(n_1 + n_2 + n_3) - n_2^3,$$

$$k_4 = -n_2n_3n_4 + n_1(n_2n_3 + n_3n_4 + n_2n_4) - n_1^2(n_2 + n_3 + n_4) + n_1^3,$$

$$k_5 = n_1n_2 + n_2n_3 + n_1n_3,$$

$$k_6 = n_1n_2 + n_2n_4 + n_1n_4,$$

$$k_7 = n_1n_3 + n_3n_4 + n_1n_4,$$

$$k_8 = n_2n_3 + n_3n_4 + n_2n_4. \tag{A3}$$

APPENDIX B

Assuming Relation 16 as the transfer matrix for the distributed element (shaft), in which rotary inertia and gyroscopic effects are considered, the main transfer matrix would have the following elements:

$$T_{11} = -\frac{e^{n_1x}n_2n_3n_4}{k_7} + \frac{e^{n_2x}n_1n_3n_4}{k_5} - \frac{e^{n_3x}n_1n_2n_4}{k_3} + \frac{e^{n_4x}n_1n_2n_3}{k_1},$$

$$T_{12} = \frac{1}{E}\left(\frac{e^{n_1x}k_{12}}{k_7} - \frac{e^{n_2x}k_{11}}{k_5} + \frac{e^{n_3x}k_{10}}{k_3} - \frac{e^{n_4x}k_9}{k_1}\right),$$

$$T_{13} = \frac{1}{EI}\left(-\frac{e^{n_1x}(n_2 + n_3 + n_4)}{k_7} + \frac{e^{n_2x}(n_1 + n_3 + n_4)}{k_5} - \frac{e^{n_3x}(n_1 + n_2 + n_4)}{k_3} + \frac{e^{n_4x}(n_1 + n_2 + n_3)}{k_1}\right),$$

$$T_{14} = \frac{1}{EI}\left(-\frac{e^{n_1x}}{k_7} + \frac{e^{n_2x}}{k_5} - \frac{e^{n_3x}}{k_3} + \frac{e^{n_4x}}{k_1}\right),$$

$$T_{21} = n_1n_2n_3n_4(-\frac{e^{n_1x}}{k_7} + \frac{e^{n_2x}}{k_5} - \frac{e^{n_3x}}{k_3} + \frac{e^{n_4x}}{k_1}),$$

$$T_{22} = \frac{1}{E}\left(\frac{n_1e^{n_1x}k_{12}}{k_7} - \frac{n_2e^{n_2x}k_{11}}{k_5} + \frac{n_3e^{n_3x}k_{10}}{k_3} - \frac{n_4e^{n_4x}k_9}{k_1}\right),$$

$$T_{23} = \frac{1}{EI}\left(-\frac{n_1e^{n_1x}(n_2 + n_3 + n_4)}{k_7} + \frac{n_2e^{n_2x}(n_1 + n_3 + n_4)}{k_5} - \frac{n_3e^{n_3x}(n_1 + n_2 + n_4)}{k_3} + \frac{n_4e^{n_4x}(n_1 + n_2 + n_3)}{k_1}\right),$$

$$T_{24} = \frac{1}{EI}\left(-\frac{n_1e^{n_1x}}{k_7} + \frac{n_2e^{n_2x}}{k_5} - \frac{n_3e^{n_3x}}{k_3} + \frac{n_4e^{n_4x}}{k_1}\right),$$

$$T_{31} = EIn_1n_2n_3n_4\left(-\frac{n_1e^{n_1x}}{k_7} + \frac{n_2e^{n_2x}}{k_5} - \frac{n_3e^{n_3x}}{k_3} + \frac{n_4e^{n_4x}}{k_1}\right),$$

$$T_{32} = I\left(\frac{n_1^2e^{n_1x}k_{12}}{k_7} - \frac{n_2^2e^{n_2x}k_{11}}{k_5} + \frac{n_3^2e^{n_3x}k_{10}}{k_3} - \frac{n_4^2e^{n_4x}k_9}{k_1}\right),$$

$$T_{33} = -\frac{n_1^2e^{n_1x}(n_2 + n_3 + n_4)}{k_7} + \frac{n_2^2e^{n_2x}(n_1 + n_3 + n_4)}{k_5} - \frac{n_3^2e^{n_3x}(n_1 + n_2 + n_4)}{k_3} + \frac{n_4^2e^{n_4x}(n_1 + n_2 + n_3)}{k_1},$$

$$T_{34} = -\frac{n_1^2e^{n_1x}}{k_7} + \frac{n_2^2e^{n_2x}}{k_5} - \frac{n_3^2e^{n_3x}}{k_3} + \frac{n_4^2e^{n_4x}}{k_1},$$

$$T_{41} = -\frac{k_8n_2n_3n_4}{k_7} + \frac{k_6n_1n_3n_4}{k_5} - \frac{k_4n_1n_2n_4}{k_3} + \frac{k_2n_1n_2n_3}{k_1},$$

$$T_{42} = \frac{1}{E}\left(\frac{k_8 k_{12}}{k_7} - \frac{k_6 k_{11}}{k_5} + \frac{k_4 k_{10}}{k_3} - \frac{k_2 k_9}{k_1}\right),$$

$$T_{43} = \frac{1}{EI}\left(-\frac{k_8(n_2+n_3+n_4)}{k_7} + \frac{k_6(n_1+n_3+n_4)}{k_5} - \frac{k_4(n_1+n_2+n_4)}{k_3} + \frac{k_2(n_1+n_2+n_3)}{k_1}\right),$$

$$T_{44} = \frac{1}{EI}\left(-\frac{k_8}{k_7} + \frac{k_6}{k_5} - \frac{k_4}{k_3} + \frac{k_2}{k_1}\right). \quad \text{(B1)}$$

In which k_1 to k_{12} are the following relation:

$$k_1 = n_1 n_2 n_3 - n_4(n_1 n_2 + n_2 n_3 + n_1 n_3) + n_4^2(n_1 + n_2 + n_3) - n_4^3,$$

$$k_2 = I(-En_4^3 + \rho(2\Omega\omega - \omega^2)n_4)e^{n_4 x},$$

$$k_3 = -n_1 n_2 n_4 + n_3(n_1 n_2 + n_2 n_4 + n_1 n_4) - n_3^2(n_1 + n_2 + n_4) + n_3^3,$$

$$k_4 = I(-En_3^3 + \rho(2\Omega\omega - \omega^2)n_3)e^{n_3 x},$$

$$k_5 = n_1 n_3 n_4 - n_2(n_1 n_3 + n_3 n_4 + n_1 n_4) + n_2^2(n_1 + n_2 + n_3) - n_2^3,$$

$$k_6 = I(-En_2^3 + \rho(2\Omega\omega - \omega^2)n_2)e^{n_2 x},$$

$$k_7 = -n_2 n_3 n_4 + n_1(n_2 n_3 + n_3 n_4 + n_2 n_4) - n_1^2(n_2 + n_3 + n_4) + n_1^3,$$

$$k_8 = I(-En_1^3 + \rho(2\Omega\omega - \omega^2)n_1)e^{n_1 x},$$

$$k_9 = E(n_1 n_2 + n_2 n_3 + n_1 n_3) + \rho(2\Omega\omega - \omega^2),$$

$$k_{10} = E(n_1 n_2 + n_2 n_4 + n_1 n_4) + \rho(2\Omega\omega - \omega^2),$$

$$k_{11} = E(n_1 n_3 + n_3 n_4 + n_1 n_4) + \rho(2\Omega\omega - \omega^2),$$

$$k_{12} = E(n_2 n_3 + n_3 n_4 + n_2 n_4) + \rho(2\Omega\omega - \omega^2). \quad \text{(B2)}$$